Journal of Physics: Condensed Matter

Magnetic order in $FeCr_2S_4$-type chalcogenide spinels

To cite this article: F J Berry *et al* 2007 *J. Phys.: Condens. Matter* **19** 266204

J. Phys.: Condens. Matter **19** (2007) 266204 (12pp) doi:10.1088/0953-8984/19/26/266204

Magnetic order in $FeCr_2S_4$-type chalcogenide spinels

F J Berry[1,6], T V Dmitrieva[2], N S Ovanesyan[2], I S Lyubutin[2], M F Thomas[3], V A Sarkisyan[2], X Ren[1], T G Aminov[4], G G Shabunina[4], V Rudenko[5], A Vorotynov[5] and Yu L Dubinskaya[2]

[1] Department of Chemistry, The Open University, Walton Hall, Milton Keynes MK7 6AA, UK
[2] A V Shubnikov Institute of Crystallography, Russian Academy of Sciences, Leninsky avenue 59, Moscow 119333, Russia
[3] Department of Physics, The University of Liverpool, Liverpool L69 3BX, UK
[4] Institute of Inorganic and General Chemistry, Russian Academy of Sciences, Leninsky avenue 31, Moscow 119907, Russia
[5] L V Kirensky Institute of Physics, Siberian Branch of Russian Academy of Sciences, Krasnoyarsk 660036, Russia

Received 14 March 2007, in final form 17 May 2007
Published 7 June 2007
Online at stacks.iop.org/JPhysCM/19/266204

Abstract

The thiospinels of composition $FeCr_2S_4$ and $Fe_{1+x}Cr_{2-2x}Sn_xS_4$ with $0 < x < 0.1$ have been examined by means of extended x-ray absorption fine structure, Mössbauer spectroscopy and magnetoresistance techniques. The structural characterization shows that tin enters the spinel-related lattice as Sn^{4+} and occupies the octahedral B site. Appreciable magnetoresistance is observed in the temperature range 160–185 K which includes the magnetic ordering temperature. The effect of slight non-stoichiometry in $FeCr_2S_4$ and of tin doping is observed in the Mössbauer spectra which show the Fe^{2+} ions to occupy the tetrahedral A sites. The Mössbauer spectra recorded around the magnetic ordering temperature are sensitive to small (0.03 T) applied magnetic fields. The influence of tin on the low temperature magnetic behaviour is associated with the distribution of Cr^{3+}, Sn^{4+} and Fe^{3+} ions around tetrahedral Fe^{2+} sites and vacancies in the anionic sublattice. An interpretation of the colossal magnetoresistance phenomena below T_N is suggested.

(Some figures in this article are in colour only in the electronic version)

1. Introduction

The discovery of colossal magnetoresistance in manganese-containing perovskites has stimulated interest in the origin of the colossal magnetoresistance (CMR) effect [1]. The effect in manganites seems to be explicable by the phenomenon of double exchange [2] and spin disorder accompanying the ferromagnetic metal to paramagnetic insulator transition. However, the existence of considerable intrinsic magnetoresistance in $FeCr_2S_4$ chalcogenide spinels [3]

[6] Author to whom any correspondence should be addressed.

which do not possess manganese, oxygen, a perovskite-related structure, or even a metal-to-insulator transition indicates that phenomena other than double exchange effects require consideration when explaining magnetoresistance in these materials.

The compound $FeCr_2S_4$ has been known as a ferrimagnet with semiconducting-like resistivity for some time [4]. It adopts a cubic normal spinel-type structure where Fe^{2+} and Cr^{3+} cations occupy tetrahedral and octahedral sites respectively [4, 5]. In contrast with $FeCr_2O_4$, which undergoes a cubic to tetragonal phase transition at T = ca 135 K, the cubic structure of $FeCr_2S_4$ is preserved at temperatures as low as 4.2 K [4]. The paramagnetic to ferrimagnetic transition occurs in the range 170–180 K [3, 4]. In the magnetically ordered state the magnetic moment of Fe^{2+} in $FeCr_2S_4$ ($\mu_{Fe} = 4.2\ \mu_B$) [4] is antiparallel to that of Cr^{3+} and the material displays a magnetic field induced quadrupole interaction below the Néel temperature [5]. However, until recently little attention has been paid to the details of the magnetic structure and changes in the lattice vibrations of $FeCr_2S_4$ in the neighbourhood of the Néel temperature. The colossal magnetoresistance effect in $FeCr_2S_4$ does not seem [3] explainable by the argument applied to the manganites via double exchange phenomena [2] and the possible role of electron–lattice coupling has been considered [6]. The possibility that lattice phenomena might be the origin of the colossal magnetoresistance effect has emerged from theoretical considerations [7] which suggest that the spin disorder transition alone cannot account for the metal-to-insulator transition observed in manganites around the Néel point. The most recent studies [8] of the interplay between magnetic order and the vibrational state of iron in $FeCr_2S_4$ have shown that ferrimagnetic order breaks down anomalously at about 20 K below the Néel temperature, and the relaxation rates of iron magnetic moments increase at about 155 K. At about 186.5 K long range magnetic order was found to develop in response to the application of a 6 T external magnetic field showing that short range magnetic order persists in $FeCr_2S_4$ well above the Néel temperature [8].

In an attempt to investigate further the magnetic properties of $FeCr_2S_4$ we have studied the material in small magnetic fields near the Néel temperature and have doped the material with tin. Although tin is non-magnetic it can experience a supertransferred magnetic hyperfine field from magnetic ions in the structure by superexchange via sulfur. We report here on the synthesis of such materials and their examination by x-ray absorption spectroscopy, ^{57}Fe and ^{119}Sn Mössbauer spectroscopy and magnetoresistance measurements.

2. Experimental techniques

Sulfur-containing spinels of formula $FeCr_2S_4$, $FeCr_{1.97}Sn_{0.03}S_4$, $Fe_{1.03}Cr_{1.94}Sn_{0.03}S_4$, $Fe_{1.05}Cr_{1.90}Sn_{0.05}S_4$ and $Fe_{1.10}Cr_{1.80}Sn_{0.10}S_4$ were prepared from appropriate mixtures of high purity elements—iron (99.9%), chromium (99.2%), sulfur (99.9%) and tin (99.9% enriched to 96% with ^{119}Sn). The mixtures, having a total weight of 1.5 g, were sealed in silica ampoules which had been evacuated to 10^{-2} Pa, heated stepwise to 910 °C over a period of five days, maintained at 910 °C for eight days and cooled to room temperature over a period of one day. In order to obtain homogeneous single-phase spinel-related structures, the samples were thoroughly ground, resealed in evacuated silica ampoules, heated to 900 °C and held at 900 °C for 11 days. The ampoules were then cooled to 650 °C and held at this temperature for one day and finally cooled to room temperature over a period of one day.

X-ray powder diffraction patterns were recorded at 298 K with a Siemens D5000 diffractometer using Cu Kα radiation. Fe K-, Cr K- and Sn K-edge x-ray absorption spectra were recorded at the synchrotron radiation source at Daresbury Laboratory UK with an average current of 200 mA at 2 GeV. The data were collected at 298 K in transmission geometry on station 7.1 (Fe and Cr edge) and station 9.2 (Sn edge). The samples were examined as pressed

discs. The edge profiles were separated from the EXAFS data and, after subtraction of linear pre-edge background, normalized to the edge step. The position of the x-ray absorption edge was defined as the energy at which the normalized absorption was 0.5 i.e., the absorption at half-height of the edge step. The EXAFS oscillations were isolated after background subtraction of the raw data using the Daresbury program EXBACK and converted into k space. The data were weighted by k^3, where k is the photoelectron wavevector, to compensate for the diminishing amplitude of EXAFS at high k. The data were fitted using the Daresbury program EXCURV98 [9].

The ^{57}Fe Mössbauer spectra were recorded with a constant acceleration spectrometer using an about 25 mCi Co/Rh source. The ^{57}Fe Mössbauer chemical isomer shift data are quoted relative to metallic iron at room temperature. The Mössbauer spectra of materials in magnetically ordered states were fitted by least-squares refinement of Lorentzian shape peaks using combined Hamiltonian fits. Overall (total) intensity, magnetic hyperfine field (H_{hf}), quadrupole shift (QS $= 1/2eQV_{zz}$), centre shift (CS), θ, angle between H_{hf} and the principal axis of the electric field gradient, ϕ, azimuthal angle of H_{hf}, and the asymmetry parameter ξ were treated as variable parameters. Relative intensities of a given hyperfine pattern assuming equal linewidths were deduced from the extracted set of hyperfine parameters. ^{119}Sn Mössbauer spectra were recorded with a $Ca^{119}SnO_3$ source and an intrinsic germanium solid state detector.

Resistivity measurements were performed by a standard four probe technique using a Quantum Design Physical Property Measurement System in the temperature range 80–300 K and an applied magnetic field up to 2 T.

3. Results and discussions

All the materials were shown by x-ray powder diffraction to be single phase.

3.1. EXAFS studies

The Fe K-edge and Cr K-edge EXAFS recorded from $FeCr_2S_4$ at 77 K showed iron to be predominantly coordinated to four sulfur atoms at a distance of 2.324 Å and chromium to be predominantly coordinated to six sulfur atoms at 2.396 Å. The results are consistent with iron adopting the tetrahedral and chromium the octahedral sites in the spinel-related structure. The Fe K- and Cr K-edge EXAFS recorded at 77 K from tin-doped $FeCr_2S_4$ were very similar with iron being coordinated by four sulfur atoms at 2.342 Å and chromium by six sulfur atoms at 2.423 Å. The Sn K-edge EXAFS showed tin to be coordinated by six sulfur atoms at 2.547 Å. The results indicate that tin substitutes for chromium on the octahedral site.

Tin K-edge x-ray absorption spectroscopy showed the x-ray absorption edge of the tin-doped variants of $FeCr_2S_4$ (29 202.2 eV) to be identical within the errors ($\pm$0.2 eV) to that of tin dioxide (29 202.1 eV) demonstrating that tin enters $FeCr_2S_4$ as Sn^{4+}.

Cr K-edge x-ray absorption spectroscopy showed $FeCr_2S_4$ to have an x-ray absorption edge at 5993.1 eV. The x-ray absorption edge of the tin-doped variants (5993.0 $\pm$ 0.2 eV) were identical showing that the incorporation of Sn^{4+} had no effect on the electron density around Cr^{3+}.

3.2. Magnetoresistance studies

The dependence of the resistance and magnetoresistance of $FeCr_2S_4$ on temperature is shown in figure 1. The results show that appreciable magnetoresistance occurs in the narrow temperature range between 165 and 182 K. A small shift of about 10 K to lower temperature in the maximum

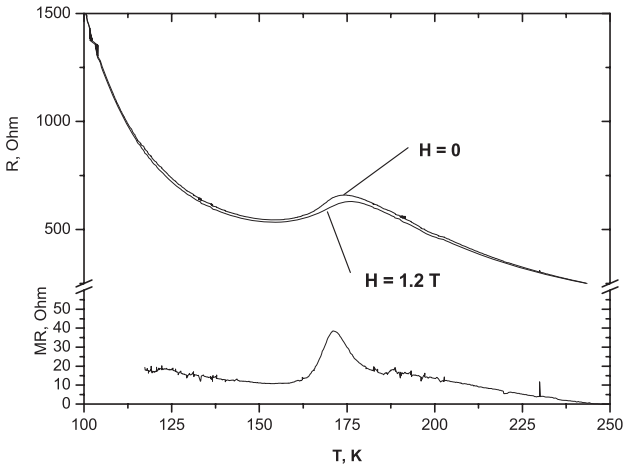

Figure 1. Temperature dependence of resistance and magnetoresistance in $FeCr_2S_4$.

Table 1. ^{57}Fe Mössbauer parameters of paramagnetic phase thiospinels. (I is the relative intensity of the subspectrum, QS is the quadrupole shift, CS is the centre shift, W is the linewidth.)

I (%)	QS (mm s^{-1})	CS (mm s^{-1})	W (mm s^{-1})
	$FeCr_2S_4$	$T = 202$ K	
12	1.18	0.65	0.34
88	0	0.65	0.32
	$Fe_{1.03}Cr_{1.94}Sn_{0.03}S$	$T = 190$ K	
27	1.24	0.65	0.41
73	0	0.66	0.58
	$Fe_{1.1}Cr_{1.8}Sn_{0.1}S_4$	$T = 200$ K	
27	0.19	0.65	0.35
17	0.54	0.64	0.31
17	0.91	0.64	0.31
18	1.22	0.64	0.31
12	1.55	0.64	0.31
6	1.95	0.64	0.31
2	2.42	0.64	0.31
1	2.67	0.92	0.35

of magnetoresistance in $FeCr_{1.97}Sn_{0.03}S_4$ and of about 4 K in $Fe_{1.03}Cr_{1.94}Sn_{0.03}S_4$ was observed to accompany tin doping.

3.3. Mössbauer spectroscopy studies

3.3.1. Thiospinels in the paramagnetic state. The ^{57}Fe Mössbauer spectra recorded from samples of $FeCr_2S_4$, $Fe_{1.03}Cr_{1.94}Sn_{0.03}S_4$ and $Fe_{1.10}Cr_{1.80}Sn_{0.10}S_4$ at temperatures between 190 and 202 K are shown in figure 2. All the spectra consist of a single line together with one or more doublets. The isomer shifts for all components are identical within the errors (table 1) and can be attributed to Fe^{2+} ions in the tetrahedral A sites of the spinel-related structure. The

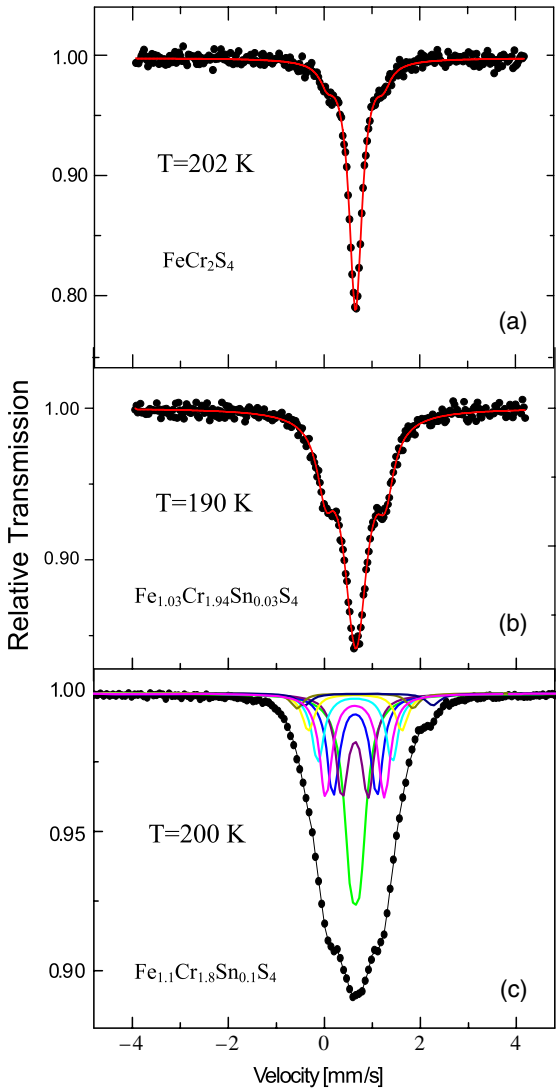

Figure 2. ^{57}Fe Mössbauer spectra recorded from samples above the magnetic ordering temperature T_N: (a) $FeCr_2S_4$ at 202 K, (b) $Fe_{1.03}Cr_{1.94}Sn_{0.03}S_4$ at 190 K, and (c) $Fe_{1.10}Cr_{1.80}Sn_{0.10}S_4$ at 200 K.

single-line absorption can be associated with the Fe^{2+} in a strictly cubic array of 12 nearest cation neighbour Cr^{3+} ions. The quadrupole split absorptions are associated with the location of Sn^{4+} ions in nearest octahedral B sublattice sites. The observation of quadrupole split components in the ^{57}Fe Mössbauer spectrum recorded from $FeCr_2S_4$, with similar Mössbauer parameters to that recorded from $Fe_{1.03}Cr_{1.94}Sn_{0.03}S_4$ endorses previous reports [8, 10] that $FeCr_2S_4$ undergoes a departure from stoichiometry with concomitant formation of an iron-rich phase of composition $Fe_{1+x}Cr_{2-x}S_4$ in which the excess iron occupies octahedral B sites and consequently leads to a non-cubic array in the B sublattice surrounding the tetrahedral Fe(A) site.

The substitution of Cr^{3+} by Sn^{4+} and the strong preference of Sn^{4+} for the octahedral B sites results in the excess Fe^{2+} ions occupying B sites according to the

formulation (Fe)$[Fe_xCr_{2-2x}Sn_x]S_4$. The Fe^{2+} component representing Fe^{2+} in the B site of $Fe_{1.1}Cr_{1.8}Sn_{0.1}S_4$ with a higher isomer shift corresponds to an intensity of less than 1% and was not amenable to fitting.

The spectrum of $Fe[Fe_{0.03}Cr_{1.94}Sn_{0.03}]S_4$, consisting of one double and one single line (figure 2(b)) representing the tetrahedral Fe^{2+}(A) sites with different B ion nearest environments, gave an area S_s of 73% for the single line and an area S_d of 27% for the doublet.

For a random cation distribution over the spinel lattice, the probability $P(k)$ for the tetrahedral Fe^{2+}(A) ion to have among the nearest octahedral B neighbours k ions of Cr^{3+} is

$$P(k) = \frac{12!}{k!(12-k)!}\left(1-\frac{z}{2}\right)^k\left(\frac{z}{2}\right)^{12-k}, \tag{1}$$

where z is the fraction of iron and tin in octahedral B sites which are the nearest neighbours of Fe(A). For $Fe[Fe_{0.03}Cr_{1.94}Sn_{0.03}]S_4$ ($z = 0.06$) these probabilities are:

$$P(12) = (0.97)^{12} = 0.694$$

$$P(11) = 12(0.97)^{11}(0.03) = 0.257$$

$$P(10) = 66(0.97)^{10}(0.03)^2 = 0.044$$

$$P(k < 9) \sim 0.1.$$

Assuming that the $P(12)$ component belongs to the single line in the Mössbauer spectra and the $P(11)$ and $P(10)$ components are responsible for the doublet, the area ratio of S_s:S_d is about 69:31. Thus, good agreement is obtained between calculated and experimental data.

It follows from figure 2(a) that the best fit of the spectrum for $FeCr_2S_4$ is also achieved with a single line and a small doublet in the ratio S_s:S_d = 88:12. According to the expression (1), this ratio corresponds to the formula $Fe_{1.02}Cr_{1.98}S_4$. The result is indicative of a non-stoichiometric material and demonstrates the sensitivity of the Mössbauer spectra to small degrees of non-stoichiometry as a result of excess iron.

At higher concentrations of tin in $Fe_{1.1}Cr_{1.8}Sn_{0.1}S_4$ the Mössbauer spectrum (figure 2(c)) was fitted to eight doublets with different intensities and quadrupole splittings in the region 0.19–2.42 mm s^{-1} which are associated with Fe^{2+}(A) having different nearest cation environments.

3.3.2. Magnetic ordering temperature. A number of studies [3, 4, 11] have reported the ferrimagnetic ordering temperature of $FeCr_2S_4$ to lie in the range 170–180 K with the actual value being sensitive to stoichiometry and the method of synthesis. The ^{57}Fe Mössbauer spectra recorded in this study between 175 and 160 K from the sample of composition $Fe_{1.02}Cr_{1.98}S_4$ are shown in the left panel of figure 3. It can be seen that the sextet indicating magnetic order develops between 175 and 165 K. A plot of the variation of magnetic hyperfine fields H_{hf} with temperature gives an ordering temperature of $T_N = (168 \pm 1)$ K for this sample. Similar sets of ^{57}Fe Mössbauer spectra recorded from the tin-doped sample of composition $Fe_{1.03}Cr_{1.94}Sn_{0.03}S_4$ gave an ordering temperature $T_N = (174 \pm 1)$ K and a series of ^{119}Sn Mössbauer spectra from the sample $Fe_{1.05}Cr_{1.90}Sn_{0.05}S_4$ gave an ordering temperature of $T_N = (177 \pm 2)$ K. In these latter spectra the ^{119}Sn nucleus senses the transferred hyperfine field of its magnetic neighbours to give the magnetic ordering transition temperature. The results illustrate that the ordering temperature T_N increases with increasing levels of tin doping.

A previous study of magnetic ordering in $FeCr_2S_4$ [8] showed that at 186.5 K, a temperature well above T_N (175 K), magnetic ordering (or drastic slowing of paramagnetic fluctuation) could be established by applying an external magnetic field of 6.0 T. In this investigation we studied the effect of a much smaller field of 0.03 T applied to the sample

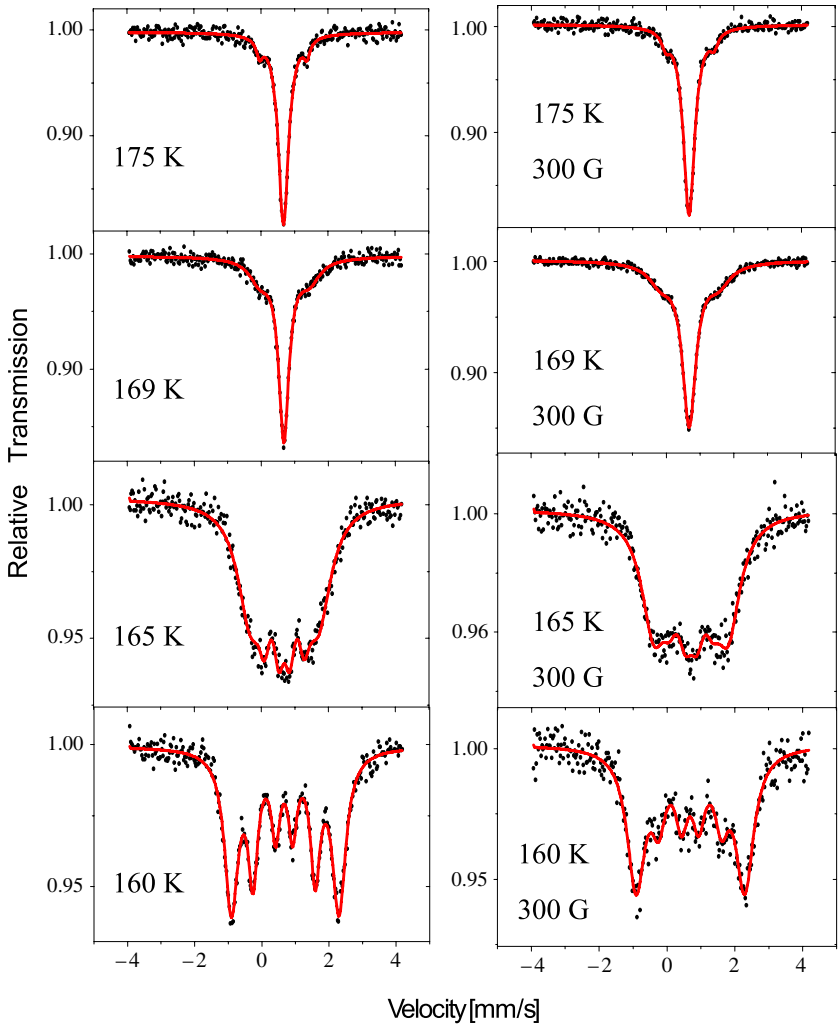

Figure 3. ^{57}Fe Mössbauer spectra of $FeCr_2S_4$ showing the effect of an applied magnetic field on the ordering. The spectra on the left are recorded in zero applied field and those on the right in a field of 0.03 T applied parallel to the gamma-ray beam.

in a direction parallel to the Mössbauer gamma-ray beam. The results are displayed in the right hand panel of figure 3. The effect of the external magnetic field on the spectra recorded at 175 and 169 K lies in the broadening of the central singlet component. At 175 K the width of this component increases from 0.30 mm s^{-1} in zero field to 0.33 mm s^{-1} when recorded in the magnetic field while at 169 K the singlet width increases from 0.30 to 0.41 mm s^{-1}. Although not dramatic, the results show that even small applied fields can influence the magnetic fluctuations in this critical temperature range. At the lower temperatures of 165 and 160 K the material is magnetically ordered and the effect of the field is in the partial alignment of the magnetic moment parallel to the gamma-ray beam (and to the applied field) and is reflected in the decrease in intensity of lines 2 and 5. The results again demonstrate that in the critical region a field as small as 0.03 T has a significant effect on the magnetic alignment.

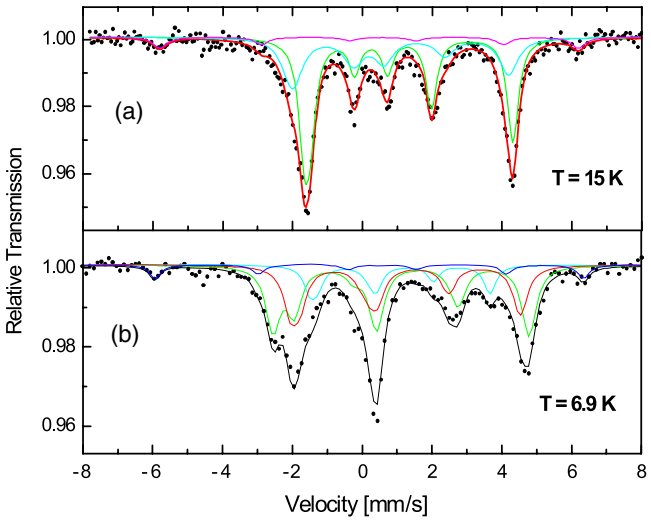

Figure 4. ^{57}Fe Mössbauer spectra of $FeCr_2S_4$ below T_N: (a) at 15 K, (b) at 6.9 K.

Table 2. ^{57}Fe Mössbauer parameters of $FeCr_2S_4$ at $T = 15$ and 6.9 K. (I is the relative intensity of the subspectrum, H_{hf} is the magnetic hyperfine field at ^{57}Fe nuclei, QS is the quadrupole shift, CS is the centre shift, W is the linewidth, θ is the polar angle between the magnetic hyperfine field H_{hf} and the principal axis of the electric field gradient EFG, ϕ is the azimuthal angle of H_{hf} and ξ is the asymmetry parameter of EFG.)

Site	I (%)	H_{hf} (T)	QS (mm s^{-1})	CS (mm s^{-1})	W (mm s^{-1})	θ	ϕ	ξ
				$T = 15$ K				
S1	57	18.6	1.08	0.78	0.38	0	0	0
S2	36	14.6	−3.06	0.53	0.64	90	0	0
S3	7	37.3	−0.38	0.38	0.48	0	0	0
				$T = 6.9$ K				
S1	46	19.4	−2.72	0.76	0.50	90	0	0.2
S4	15	13.6	−1.98	0.73	0.42	90	0	0
S2	33	17.1	−2.64	0.79	0.51	90	0	0
S3	6	38.2	−0.38	0.38	0.39	0	0	0

3.3.3. Magnetically ordered states at low temperatures. It has been established that the electronic state of the Fe^{2+} ions on the tetrahedral A sites of the spinel-related structure undergo a transition at T_{tr} about 10 K that results in the angle between the principal axis of the electric field gradient, V_{zz}, and the magnetic hyperfine field, H_{hf}, changing from a higher temperature value of $\theta = 0°$ to a low temperature value of $\theta = 90°$ [11]. This occurs without any observable change in the cubic structure [4]. This change in our study of $FeCr_2S_4$—seen from the analysis of figure 2(a) to be better represented as $Fe_{1.02}Cr_{1.98}S_4$—is illustrated in figure 4 where the upper spectrum, figure 4(a), was recorded at 15 K (i.e. above T_{tr}) whilst the lower spectrum figure 4(b), was recorded at 6.9 K (i.e. below T_{tr}). The parameters of the fits to these spectra are contained in table 2.

The excess iron modifies the spectrum recorded from the stoichiometric compound fitted by a single component [11, 12] in two ways. The excess iron occupies octahedral B sites in the spinel-related structure where it assumes an Fe^{3+} state which gives rise to component S3 of

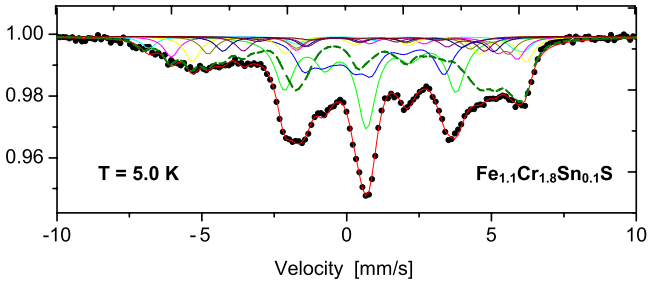

Figure 5. ^{57}Fe Mössbauer spectrum recorded from $Fe_{1.10}Cr_{1.80}Sn_{0.10}S_4$ at 5 K.

Table 3. ^{57}Fe Mössbauer parameters of $Fe_{1.1}Cr_{1.8}Sn_{0.1}S_4$ at $T = 5$ K. (I is the relative intensity of the subspectrum, H_{hf} is the magnetic hyperfine field at ^{57}Fe nuclei, QS is the quadrupole shift, CS is the centre shift, W is the linewidth, θ is the polar angle between the magnetic hyperfine field H_{hf} and the principal axis of the electric field gradient EFG, ϕ is the azimuthal angle of H_{hf} and ξ is the asymmetry parameter of EFG.)

I (%)	H_{hf} (T)	QS (mm s^{-1})	CS (mm s^{-1})	W (mm s^{-1})	θ	ϕ	ξ
30	11.7	−2.87	0.75	0.78	51	90	0.7
22	9.5	−2.54	0.75	0.78	72	90	0.5
4	41.1	−2.50	0.82	0.62	0.1	0	0.2
9	37.4	−1.84	0.82	0.62	0.1	0	0.2
10	36.0	−0.85	0.82	0.62	0.1	0	0.2
9	32.4	−0.86	0.82	0.62	0.1	0	0.2
7	29.1	−0.84	0.82	0.62	0.2	0	0.2
6	25.9	−0.46	0.82	0.62	0.2	0	0.2
2	23.2	−0.27	0.82	0.62	0.9	0	0.2

table 2 and manifests itself in the spectrum of figure 4(a) by peaks at ∼+6 and ∼−6 mm s^{-1}. The occupation of some B sites with Fe^{3+} rather than Cr^{3+} ions changes the state of Fe^{2+} ions on neighbouring A sites to give rise to component S2 while the main component S1 has similar parameters to those of stoichiometric $FeCr_2S_4$ and derives from Fe^{2+} ions on unperturbed A sites.

The spectrum in figure 4(b) at 6.9 K is fitted to four components. Relating these to the fit at 15 K it is seen that the Fe^{3+} component S3 remains the same, the component S1 at 15 K transforms to the sum of S1 and S4 at 6.9 K, and the component S2 at 15 K transforms to S2 at 6.9 K. The most prominent feature, the change in sign of the quadrupole interaction of the main component (S1) and of the polar angle θ from 0° to 90°, could not occur without some structural rearrangement even though no departure from cubic symmetry has been detected by neutron and x-ray diffraction measurements. The reversal in the sign of the quadrupole interaction for Fe^{2+} in tetrahedral sites suggests the reversal of the ground state term of the lower energy doublet from $d_{x^2-y^2}$ at 15 K to d_{3z^2-1} at 6.9 K. An antiferrodistortive phase transition as revealed by a lambda-type peak in the heat capacity–temperature curve has been suggested [13]. However it is difficult to explain the persistence of the cubic structure for powder samples below the transition temperature.

The effects of non-stoichiometric variations on the parent compound $FeCr_2S_4$ have already received some attention [14, 15]. In our study, the effect of tin doping on magnetic order in $Fe_{1.10}Cr_{1.80}Sn_{0.10}S_4$ at 5.0 K is shown in figure 5. The ^{57}Fe Mössbauer parameters are listed in table 3. The overall shape of the spectrum corresponds to that shown in figure 4(b) indicating

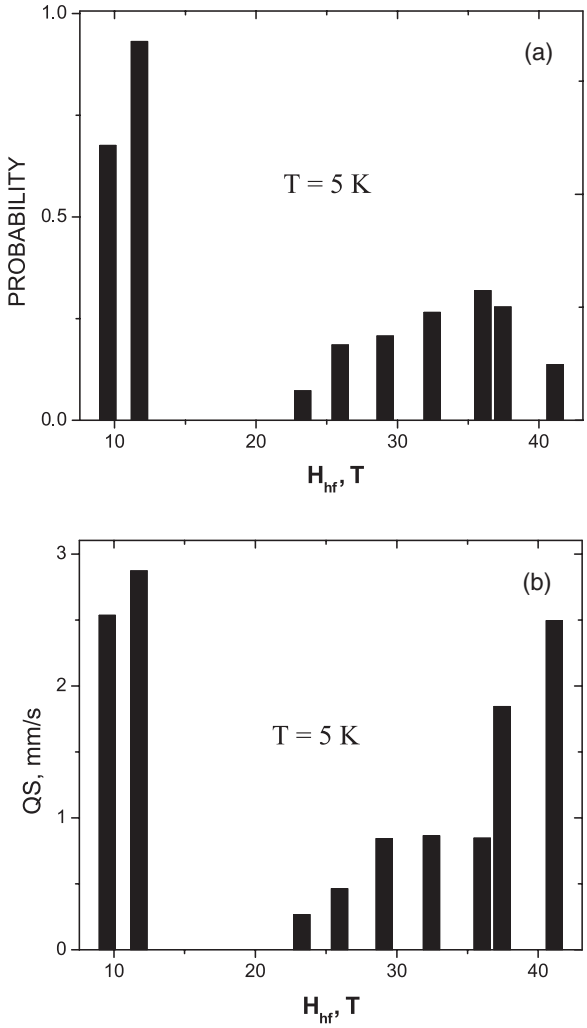

Figure 6. Distributions of hyperfine parameters from the fit of the spectrum in figure 5. (a) shows the distribution of magnetic hyperfine fields at iron nuclei in $Fe_{1.10}Cr_{1.80}Sn_{0.10}S_4$, (b) shows the correlation between H_{hf} and QS.

that it arises from the phase that exists below the transition temperature T_{tr}. However, in comparing the two spectra, it is seen that the spectrum recorded from the tin-doped material shows a broad range of absorption at velocities $<$ca -3.0 mm s^{-1} and another broad region of absorption underlying the peaks at velocities $>$ca 3.0 mm s^{-1}. The spectrum recorded from the sample $Fe_{1.10}Cr_{1.80}Sn_{0.10}S_4$ in figure 5 was fitted using a multi-component approach. The broad high field distribution was constrained to the same variable value of centre shift, polar and azimuthal angles and asymmetry parameter. It is seen that the increased and broadened distribution of high magnetic field components occurs with tin substitution. The distribution of hyperfine fields (H_{hf}) and its correlation with quadrupole interaction values are shown in figure 6. It is seen from table 3 that the two most intense magnetic components have intermediate values of polar angle and lower values of H_{hf} compared with the main components of the spectrum recorded from $FeCr_2S_4$. It is difficult to explain the large distribution in values

of H_{hf} and quadrupole interaction (figure 6) solely in terms of a random distribution of Cr^{3+}(B), Sn^{4+}(B) and Fe^{2+}(B) ions over the nearest cation neighbour sites of the Fe^{2+}(A) ions. It would be reasonable to assume that a certain number of structural defects (vacancies) exist in the anion sublattice. This could lead to the disruption of Fe^{2+}(A)–S–M(B) bonds (M = Cr, Fe, Sn) and the distortion of the local environment of Fe^{2+}(A) ions. This would result in a significant change of the orbital contribution to H_{hf} and the existence of two sets of magnetic hyperfine fields near 10 T and at ca 30–40 T—(figure 6(b)) may result from distinct values of the orbital contribution depending on the character of local distortions. However, the subdivision of Mössbauer spectra at low temperature into two different sets of hyperfine patterns remains a challenge. By comparison with the low intensity high field magnetic component recorded from pure $FeCr_2S_4$, we suggest that the broad high field distribution in the spectrum recorded from the tin-substituted material corresponds to an increased amount of iron and tin atoms in near neighbour octahedral sites. The two narrow lower field magnetic components would correspond to a less perturbed configuration close to that of pure $FeCr_2S_4$.

4. A model for CMR phenomena below T_N

The interest in the compound $FeCr_2S_4$ lies in its pronounced magnetoresistance in the temperature range 160–185 K.

As a result of intersublattice antiferromagnetic Fe^{2+}–S–Cr^{3+} exchange interaction a long range magnetic order is established. The conducting properties of the material are probably related to the extra e_g electron of high spin Fe^{2+} which is capable of delocalization into free Cr^{3+} orbitals due to a significant sharing of covalent bonding with intermediate sulfur anions. The change of the conductivity type from semiconducting to metallic at the transition from the paramagnetic to magnetically ordered state may be related to a spin polarization since electron transfer occurs without spin flop. It would then be reasonable to expect that the metallic state will be retained when the temperature decreases. Since the metallic state is maintained only in a small temperature range below the Néel temperature it would seem that at the transition into the magnetically ordered state a significant ferromagnetic component of intersublattice exchange is gradually suppressed by the main antiferromagnetic component with decreasing temperature. A parallel orientation of electron spins promotes a gapless (metallic) conductivity of electrons with polarized spin as in the ferromagnetic and metallic compound $CuCr_2S_4$. For this compound the ferromagnetic intersublattice interaction occurs between t_{2g} unpaired electrons of Cr^{3+} and Cu^{2+}. It is likely that an analogous contribution to a ferromagnetic part of exchange exists in the case of $FeCr_2S_4$. The external magnetic field would intensify a ferromagnetic exchange and, respectively, increase the metallic conductivity. At lower temperature the ferromagnetic component of the exchange interaction is suppressed by the antiferromagnetic interaction and magnetoresistance disappears. The magnetic relaxation effect observed in the Mössbauer spectra [8] in a wide temperature range below T_N (of about 30 K) indirectly supports this explanation. Hence we envisage ferromagnetic order just below the ordering temperature with Fe^{2+} moments parallel to Cr^{3+} in a narrow temperature range where CMR exists. At lower temperatures antiparallel orientation of the moments occurs with cessation of CMR effects.

We would suggest that the experimental validation of the above assumption may be realized using Mössbauer spectroscopy over a wide temperature range. The application of an external magnetic field would be required to determine the sign of hyperfine magnetic field at iron nuclei. A change in the sign of the field at the iron nuclei at temperatures where CMR is observed would provide evidence of such a mechanism and we plan to perform such experiments and report on them in a subsequent paper.

Acknowledgments

This work was supported by the Russian Foundation for Basic Research (grant 05-02-16142-a), by the Programme of the Russian Academy of Sciences under the project: 'Strongly Correlated Electronic Systems' and by The Royal Society (Short Term Visit Grant).

References

[1] Helmolt R, Wecker J, Holzapfel B, Schultz L and Samwer K 1993 *Phys. Rev. Lett.* **71** 2331
[2] Zener C 1951 *Phys. Rev.* **87** 403
[3] Ramirez A P, Cava R J and Krajewski J 1997 *Nature* **386** 156
[4] Shirane G, Cox D E and Pickart S J 1964 *J. Appl. Phys.* **35** 954
[5] Yagnik C M and Mathur H B 1967 *Solid State Commun.* **5** 841
[6] Eibschutz M, Shtrikman S and Tenenbaum Y 1967 *Phys. Lett.* A **24** 563
[7] Hoy G R and Singh K P 1968 *Phys. Rev.* **172** 514
[8] Klencsar Z, Kuzmann E, Homonnay Z, Vertes A, Simopoulos A, Devlin E and Kallias G 2003 *J. Phys. Chem. Solids* **64** 325
[9] Binstead N 1998 EXCURV98 (CCLRC Daresbury Laboratory Computer Program)
[10] Brossard L, Dormann J L, Goldstein L, Gibart P and Renaudin P 1979 *Phys. Rev.* B **20** 2933
[11] Spender M R and Morrish A H 1972 *Solid State Commun.* **11** 1417
[12] Yang Z, Tan S and Zhang Y 2000 *Solid State Commun.* **115** 679
[13] van Diepen A M, Lotgering F K and Olijhoek J F 1976 *J. Magn. Magn. Mater.* **3** 117
[14] Li Q, Zang J, Bishop A R and Soukoulis C M 1997 *Phys. Rev.* B **56** 4541
[15] Gibart P, Goldstein L and Brossard L 1976 *J. Magn. Magn. Mater.* **3** 109